IUST
Iran University of Science and Technology

Iranian Journal of Electrical and Electronic Engineering

Journal Homepage: ijeee.iust.ac.ir

Research Paper

Enhancing Voltage Regulation in DC Microgrids Using a Price Incentive Load Management Approach

A. Karimpour*(C.A.), A. M. Amani**, M. Karimpour***, and M. Jalili**

Abstract: This paper studies the voltage regulation problem in DC microgrids in the presence of variable loads. DC microgrids generally include several Distributed Generation Units (DGUs), connected to electrical loads through DC power lines. The variable nature of loads at each spot, caused for example by moving electric vehicles, may cause voltage deregulation in the grid. To reduce this undesired effect, this study proposes an incentive-based load management strategy to balance the loads connected to the grid. The electricity price at each node of the grid is considered to be dependent on its voltage. This guide moving customers to connect to cheaper connection points, and ultimately results in even load distribution. Simulations show the improvement in the voltage regulation, power loss, and efficiency of the grid even when only a small portion of customers accept the proposed incentive.

Keywords: DC Microgrid, Voltage Regulation, Load Management, Variable Energy Price.

1 Introduction

IN recent years, environmental issues have encouraged the uptake of renewable energy courses for electricity generation [1]. In this context, microgrids as the building blocks of modern power systems have emerged, in which Distributed Energy Resources (DERs), Energy Storage Systems (ESS) and generators supply local loads over Medium or low voltage grids [2, 3]. Microgrids can increase the efficiency and power quality of the grid [4], enhance the local resiliency against faults and improve the peak shaving capability [5].

Microgrids are able to operate in either grid-connected or islanded modes [6]. Although this concept originated in AC power systems, recent investigations show that DC microgrids can work more efficiently than AC microgrids [7]. DC microgrids offer advantages, such as reduction of DC-AC conversion losses, no need to frequency control, overcoming frequency synchronization, solving the unbalanced electric signals issue, incorporating no reactive power, no harmonics, and no skin effect. DC microgrids have been applied in avionics, automotive and marine industries as well as residential energy systems.

Efforts on reliable operations of DC microgrids have raised some technical challenges, among them, current sharing and voltage balancing are important from a control engineering perspective. These problems can be solved independently in AC microgrids because of their different nature [8]. However, the current sharing forces some constraints on the nodes' voltage in a DC microgrid, which makes their independent control a challenge.

Some load sharing algorithms in DC microgrids distribute the total load among all sources proportional to their capacity [9-14]. However, different energy prices of dispatchable (gas turbine) and non-dispatchable (wind turbine) sources may force the designer to use other algorithms, such as dynamic economic dispatch [2]. Those algorithms inspired by a droop controller concept in AC systems have been developed for economic power dispatch in DC

Iranian Journal of Electrical and Electronic Engineering, 2021.
Paper first received 02 November 2020, revised 19 April 2021, and accepted 21 April 2021.
* The author is with the Electrical Engineering Department, Ferdowsi University of Mashhad, Mashhad, Iran.
E-mail: karimpor@um.ac.ir.
** The authors are with the School of Engineering, RMIT University, Melbourne, VIC 3001, Australia.
E-mails: ali.moradiamani@rmit.edu.au and mahdi.jalili@rmit.edu.au.
*** The author is with the School of Engineering, University of Melbourne, Melbourne, Parkville, 3010, Australia.
E-mail: mkarimpour@student.unimelb.edu.au.
Corresponding Author: A. Karimpour.
https://doi.org/10.22068/IJEEE.17.4.2024

microgrids [15]. Advanced control algorithms, such as consensus-based [16] and sliding mode controllers, have also been proposed [9]. Although a centralized control scheme has been applied to solve the current sharing and voltage balancing problems in DC microgrids [10, 11], distributed control algorithms, based on local measurements at the so-called Point of Common Coupling (PCC), are practically desired [10], [12-14], [16-18]. Most of the existing research activities rely on a reduced-order model of microgrids derived using the Kron reduction algorithm [19, 20]. This model consolidates all interim consumption nodes into the generation points and results in a low-dimensional model of the grid. Although the simplified model makes the analysis of the complicated system feasible, some problems with consumption nodes, such as excessive voltage drop, may be neglected. As another simplification, the strategy proposed in [14] ignores the resistance of the RLC filter. Under this situation the authors derived weighted voltage balance, that cannot be derived with a complete filter model.

Although, there is a conflicting goal between current sharing and voltage regulation in a DC microgrid. The two objectives, including either tuning voltages tightly or decreasing current sharing errors considered in [21], solve the challenge, by a compromised control conception between current sharing and voltage regulation to balance the trade-off and satisfy different requirements.

Weighted voltage balance had been mentioned in the literature many times since suitable voltage regulation is not accessible due to its interaction with the current sharing. Although weighted voltage is achievable but it needs the exact knowledge of almost all network parameters (see Lemma 1 [10]). However, with some simplification such as ignoring the resistance of the RLC filter, weighted voltage regulation can be derived with only knowledge of DGUs currents connected through communication links [14]. Weighted voltage regulation mentioned in the literature is usually based on Kron reduction in which the consumption nodes (node without a DGU) are absorbed. That is, in this situation weighted voltage regulation does not guarantee the suitable value on consumption nodes.

To tackle the above-mentioned drawbacks and derive a more suitable voltage regulation, a new criterion to check the node voltages was proposed. In addition, to use the potential sensitivity of the proposed criterion to load distribution, demand-side management strategy was used to manage the node voltages at an acceptable value.

Demand-side management was previously used in [22] to provide setpoints for each generation unit. Ref. [23] use demand-side management for control of microgrids. To tackle the solar renewable uncertainty of sources, demand response programs were used in [24]. Ref. [25] use demand-side management to minimize the operation cost and maintain the power balance. In this study, we used demand response to improve the voltage profile.

This study aims to improve the voltage regulation, particularly in the consumption nodes, through a price-based incentive method. A complete filter model was considered, that can maintain the current sharing. In our proposed method, the electrical vehicles (EVs) were considered as moving consumers in a DC microgrid. The main contributions of this paper are summarized as below:

- A load management method is proposed that can lead to more suitable voltage regulation and will maintain the current sharing among DGUs;
- The proposed method can improve the voltage regulation, reduce the power losses in the network, and increasing the efficiency of the microgrid;
- A different measure ($f_{max-min}$) to consider the voltage regulation in DC microgrids is proposed;
- A complete model for RLC filter considered;
- Consumption node voltages are considered as well as DGUs node voltages;
- The proposed method is designed such that the average price does not change for customers.

The potential of EVs in changing their charging position is used that can improve voltage regulation.

The remainder of this paper is organized as described herein. Section 2 provides a comparison between centralized, decentralized, and distributed control schemes. Particularly, we emphasize how the distributed scheme is able to control the current sharing in DC microgrids. In Section 3, the model of the microgrid is presented. The control problem is formulated in Section 4 and the relationship between voltage regulation and current sharing are presented. In Section 5 the simulation results are illustrated and discussed. Finally, conclusions and recommendations for future research are provided.

2 Centralized, Decentralized, and Distributed Control

From an implementation perspective, control systems are categorized into centralized, decentralized, and distributed control schemes. In the centralized approach, all data from sensors are gathered in a central controller where the control algorithm is performed and the resulted control commands are sent back to actuators. A rich literature in the design of centralized control systems has been developed for decades. For example, economic dispatch in conventional power systems is an application of this scheme. However, practical drawbacks such as limitations in scalability, communication delays, and having a single point of failure make it not suitable for large-scale systems [26].

To address these problems, distributed control systems were introduced, in which, controllers are distributed throughout the system. Each controller applies a local control algorithm using its local information or data

from other subsystems. A central system may be needed for supervisory control or other coordination. Algorithms for designing distributed controllers are often more complex than those for the centralized ones. However, because of clear advantages, such as reliability, cost reduction, and scalability [26], large-scale processes have been gradually moving towards distributed control systems. The decentralized control scheme is a specific type of distributed control where each controller relies only on its local data to implement the control algorithm. In other words, no communication network among controllers is required [27, 28]. Droop control, which is normally implemented in AC generation systems, is an example of decentralized control systems. Although decentralized control may overcome all the aforementioned drawbacks of centralized control, the possibility of achieving control objectives optimally robustly is always a question. Recently, several distributed control systems have been proposed to achieve current sharing and voltage balancing in DC microgrids [10], [12-14], [16-18]. In this study, we propose a technique to improve the performance of the distributed control scheme suggested in [14] in DC microgrids with moving consumers, such as EVs.

3 Model of a DC Microgrid

Each DGU in a DC microgrid includes a DC voltage source (e.g. solar cells) connected to grid through a buck converter and an RLC filter, as shown in Fig. 1. The line connecting nodes *i* and *j* of the grid is modeled as a resistance ($R_{ij} > 0$) in series with an inductance ($L_{ij} > 0$). I_{loadi} shows the local load, for example, an EV, which is supplied by *i*-th DGU.

The dynamical behavior of each DGU (see Fig. 1) can be represented as with the following two states: the current flow in the filter inductance L_i and the voltage across filter capacitance C_i. The state-space model representing *i*-th DGU is given by

$$L_i \dot{I}_i = -V_i - R_i I_i + u_i \tag{1}$$

$$C_i \dot{V}_i = I_i - I_{loadi} - \sum_{j \in x_i} I_{ij} \tag{2}$$

where V_i is the voltage at PCC_i, I_i is the current generated by DGU_i, I_{loadi} is load current at PCC_i, I_{ij} is the current flowing over the *ij*-th line, χ_i is the set of DC lines connected to the PCC_i and u_i is the output of the buck converter of DGU_i which can be considered as the control signal.

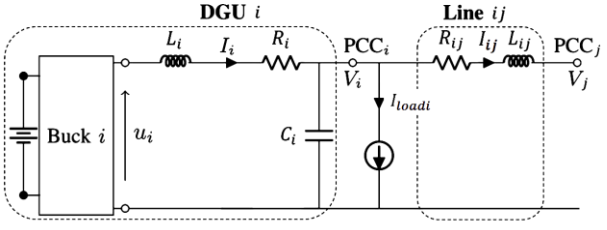

Fig. 1 Electrical scheme of DGU_i connected to PCC_i and line connected PCC_i to PCC_j.

Dynamical equation showing the energy transfer over the *ij*-th line is

$$L_{ij} \dot{I}_{ij} = V_i - V_j - R_{ij} I_{ij} \tag{3}$$

Therefore, state space equations describing the overall behavior of a DC microgrid read as,

$$L\dot{I} = -V - RI + u \tag{4}$$

$$C\dot{V} = I - I_{load} + ßI_L \tag{5}$$

$$L_l \dot{I}_L = -ß^T V - R_l I_L \tag{6}$$

where R, C, R, $\in R^{n\times n}$, R_l, $L_l \in R^{m\times m}$ are diagonal matrices, I, I_{load}, V, $u \in R^n$, $I_l \in R^m$, n is the number of DGUs, and m is the number of DC lines. $ß \in R^{n\times m}$ is the incidence matrix of network and is defined by

$$ß_{ij} = \begin{cases} +1 & \text{if } j\text{-th line withdraws current from node } i \\ -1 & \text{if } j\text{-th line injects current to node } i \\ 0 & \text{if } j\text{-th line is not connected to node } i \end{cases}$$

4 Price-Based Incentive Load Management Approach

In a perfect load sharing in DC microgrids, the load assigned to *i*-th DGU is proportional to its generation capacity, which we show it by w_i^{-1} here. The desired steady-state current of *i*-th DGU is shown by $w_i^{-1} i^*$, where i^* is the total load current divided by the total generation capacity of all DGUs in the microgrid,

$$i^* = \frac{\sum_{i=1}^{n} I_{load}(i)}{\sum_{i=1}^{n} w_i^{-1}} = \frac{\mathbb{I}_n^T I_{load}}{\mathbb{I}_n^T W^{-1} \mathbb{I}_n} \tag{7}$$

where $W = \text{diag}\{w_1, w_2, \ldots, w_n\}$ and $\mathbb{I}_n \in R^n$ is an all-one vector. The proportional current sharing objective is

$$\lim_{t\to+\infty} I(t) = W^{-1}\mathbb{I}_n \frac{\mathbb{I}_n^T I_{load}}{\mathbb{I}_n^T W^{-1} \mathbb{I}_n} \tag{8}$$

Remark 1: Note that by setting all w_is to be identical, the total current demand is equally shared among all DGUs, while by assigning different values for w_i the currents can be shared arbitrarily among DGUs.

To derive a distributed control structure for a proportional current sharing, an undirected and connected communication network among all DGU nodes is considered [10]. Distributed control scheme that we use in this paper is in accordance with [14]. To achieve a proportional current sharing, it is necessary that, $w_i I_i = w_j I_j$ for any *i*, *j* in the set of DGU nodes. Ref. [14] considers the following distributed controller at *i*-th

node,

$$T_{\theta i}\dot{\theta}_i = -\sum_{j\in N_i^{com}} \gamma_{ij}\left(w_i I_i - w_j I_j\right) \quad (9)$$

$$T_{\phi i}\dot{\phi}_i = -\phi_i + I_i \quad (10)$$

$$u_i = -K_i\left(I_i - \phi_i\right) + w_i \sum_{j\in N_i^{com}} \gamma_{ij}\left(\theta_i - \theta_j\right) + V_i^* \quad (11)$$

where $T_{\theta i}$, $T_{\varphi i}$, $K_i \in R^+$ are tuning parameters, V_i^* is the reference voltage of node i, N_i^{com} is the set of neighbors of node i, i.e. nodes connected to node i via a communication link, and γ_{ij} shows the weight of edge ij. The overall control scheme can be written as

$$T_\theta\dot{\theta} = -L^{com}WI \quad (12)$$

$$T_\phi\dot{\phi} = -\phi + I \quad (13)$$

$$u = -K\left(I - \phi\right) + WL^{com}\theta + V^* \quad (14)$$

$$L^{com} = ß^{com}\Gamma ß^T \quad (15)$$

where T_θ, T_φ, $K \in R^{n\times n} > 0$ are positive definite diagonal matrices, and $ß^{com}$ is incidence matrix of communication graph and Γ is a positive definite diagonal matrix describing the weights on the edges. L^{com} is the weighted Laplacian matrix associated with the communication network. Augmenting the microgrid model with the distributed controller leads to the following equations:

$$L\dot{I} = -V - RI - K\left(I - \phi\right) + WL^{com}\theta + V^* \quad (16)$$

$$C\dot{V} = I - I_{load} + ßI_L \quad (17)$$

$$L_l\dot{I}_L = -ß^T V - R_l I_L \quad (18)$$

$$T_\theta\dot{\theta} = -L^{com}WI \quad (19)$$

$$T_\phi\dot{\phi} = -\phi + I \quad (20)$$

The formulation used in this study ((16)-(20)) is similar to what was used in the literature [14]. However, the passive term RI in (16) is a new term used in this study. Therefore, using Lemma 1 and Theorem 1 of [14], one can derive the existence of a steady-state solution and perform the stability analysis.

Remark 2: The weighted average voltage regulation algorithm derived in [14] results in,

$$\lim_{t\to+\infty} \mathbb{I}_n^T W^{-1}V\left(t\right) = \mathbb{I}_n^T W^{-1}V^* \quad (21)$$

the following lemma shows that if RI is considered, the weighted average algorithm proposed in [14] does not necessarily result in a voltage regulation in DC microgrids.

Lemma 1- Weighted average voltage regulation: The weighted average voltage in the microgrid modeled by (16)-(20) is strictly less than the weighted average reference voltage. That is,

$$\lim_{t\to+\infty} \mathbb{I}_n^T W^{-1}V\left(t\right) = \mathbb{I}_n^T W^{-1}\hat{V} < \mathbb{I}_n^T W^{-1}V^* \quad (22)$$

where $\hat{V}$ is the steady-state value of node voltages.

Proof: Steady-state values of (16) and (20) are

$$0 = -\hat{V} - R\hat{I} - K\left(\hat{I} - \hat{\phi}\right) + WL^{com}\hat{\theta} + V^* \quad (23)$$

$$0 = -\hat{\phi} + \hat{I} \quad (24)$$

where $\hat{\phi}$, $\hat{I}$, and $\hat{\theta}$ are the steady-state values of φ, I, and θ, respectively. By multiplying both sides of (23) by $\mathbb{I}_n^T W^{-1}$ and using (24), one can derive

$$\mathbb{I}_n^T W^{-1}\hat{V} = -\mathbb{I}_n^T W^{-1}R\hat{I} + \mathbb{I}_n^T L^{com}\hat{\theta} + \mathbb{I}_n^T W^{-1}V^*$$

The zero-column-sum feature of the Laplacian matrix of undirected network results in $\mathbb{I}_n^T WL^{com} = 0$. Thus,

$$\mathbb{I}_n^T W^{-1}\hat{V} = -\mathbb{I}_n^T W^{-1}R\hat{I} + \mathbb{I}_n^T W^{-1}V^*$$

We have the following inequality when resistors of RLC filters are considered, which completes the proof.

$$\mathbb{I}_n^T W^{-1}\hat{V} < \mathbb{I}_n^T W^{-1}V^* \quad ■$$

In this study, we consider the max-min function $f_{max\text{-}min}(V):R^n\rightarrow R^+$

$$f_{\max-\min}\left(V\right) = \max\left(V\right) - \min\left(V\right) \quad (25)$$

as a measure of the quality of voltage regulation. $max(V)$ ($min(V)$) is the largest (smallest) element of the vector V. The max-min function, measures the deviation of the elements of a vector. This measure applies to node voltages of the original system and its lower (greater) value indicates that the voltage profile of microgrids is closer to (farther from) each other.

The following lemma shows that for a specific load and a current sharing algorithm, the reduction of the steady-state voltage deviation in nodes, i.e. $f_{max\text{-}min}(\hat{V})$, is not possible by control of the output of the buck converter u_i only.

Lemma 2- Steady-state voltage deviation control: The steady-state voltage deviation of a microgrid ($f_{max\text{-}min}(\hat{V})$), under a specified current sharing algorithm, cannot be regulated using u_i.

Proof: In the steady-state condition, (5) and (6) become

$$0 = \hat{I} - I_{load} + ß\hat{I}_L$$

$$0 = -ß^T\hat{V} - R_l\hat{I}_L$$

which lead to

$$ßR_L^{-1}ß^T\hat{V} = \hat{I} - I_{load} \quad (26)$$

where $ßR_L^{-1}ß^T$ is the Laplacian matrix of the electrical graph. The range space of this matrix is the subspace

composed by all vectors with zero average, and its null space is the subspace spanned by the all-one vector [13]. Since $\hat{I} - I_{load}$ is a vector with zero average, the set of all solutions of (26) is [29]:

$$\hat{V} = V_p + \alpha \mathbb{I}_n$$

where V_p is any solution of (26) and α is any real number. So, we have,

$$\begin{aligned} f_{\max-\min}(\hat{V}) &= \max(V_p + \alpha\mathbb{I}_n) - \min(V_p + \alpha\mathbb{I}_n) \\ &= (\max(V_p) + \alpha) - (\min(V_p) + \alpha) \\ &= \max(V_p) - \min(V_p) = f_{\max-\min}(V_p) = \text{cte.} \quad \blacksquare \end{aligned}$$

Lemma 1 shows that in a complete RLC filter, weighted voltage balance cannot be derived through distributed control mentioned in [14]. On the other hand, controlling the buck converter only does not improve the voltage deviation based on Lemma 2. Therefore, we need a new approach to tackle this problem.

To improve the voltage regulation when the resistance of filters is also considered, we propose a new incentive strategy. It states that the electricity price at each node depends on its voltage. That is, energy is more expensive in nodes with rather high voltage drops than other nodes. Therefore, if the voltage drops at one spot, because of connecting multiple EVs for example, results in a higher price, new customers look for other nodes offering cheaper prices to connect their EV. This ultimately results in a suitable voltage regulation in the microgrid. Suppose A is the nominal energy price of a microgrid. The energy price at i-th node of the system is shown by $\hat{A}_i^{new}$, as

$$\hat{A}_i^{new} = \hat{A} / (1 - \alpha \delta v_i) \tag{27}$$

$$\delta v_i = (v_i^* - v_i) / v_i^* \tag{28}$$

where δv_i is the normalized voltage drop in i-th node, $\hat{A}$ is the corrected energy price, and $\alpha \in [0, 5]$ is the tuning parameter. To shed more light on the effect of different α on the nodal prices, the per-unit nodal price $(1/(1-\alpha\delta v_i))$ is plotted against different voltage drop in Fig. 2. In this figure, larger α corresponds to a larger price deviation and for $\alpha = 0$ all prices are the same.

Remark 3: For the defined system we consider non-zero resistance of the RLC filter, therefore, all voltage drops according to (28) are positive.

Remark 4: Although according to Fig. 2, all per-unit prices are more than one, $\hat{A}$ is the base price and will be corrected such that the total income of DGUs remains constant (see (29)).

The value of α can be designed according to the customers' purchasing behavior and also the maximum and minimum allowable prices in the market. So, it can be tuned by trial and error.

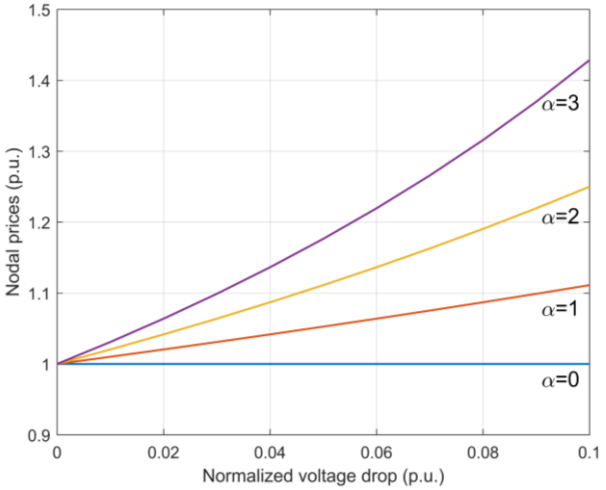

Fig. 2 Perunit nodal price versus normalized voltage drop with α as parameter (Eq. (27)).

$\hat{A}$ is the corrected energy price, which is calculated daily (weekly). B is considered as the total income received by selling the energy with the new price minus the total income received by selling with the real price in a day (week). The corrected energy price is defined in (29).

$$\hat{A} = A - B / C \tag{29}$$

where C is the total energy sold in the previous day (week). Node-specific energy price is a strong incentive to manage the system loads. The distribution of system loads to the appropriate position will lead to better voltage regulation through the system. Furthermore, it will lead to a reduction in power loss and an increase in the efficiency of the system.

In this paper and other recent papers in the literature, it is considered that most of the loads are manageable and can be optimally assigned to achieve suitable current sharing and voltage regulation. However, in every grid there might be some loads which are not manageable. Future investigation of this work could be consideration of the penetration rate of the manageable loads in the grid and how to tackle the problem of voltage regulation with the existence of other fast response sources such as battery energy storage systems (BESS).

5 Simulation Results

Consider a DC microgrid with four DGUs interconnected through 10 power lines and 7 EV loads, as shown in Fig. 3. We apply our proposed incentive-based load management developed in (27)-(29) on the distributed consensus algorithm. Parameters of DGUs and the line parameters are reported in Tables 1 and 2, respectively. Each PCC supply a local DC load (here, EV fleet), which can be considered as price-sensitive loads. The weights associated with the communication graph are identical (set at 2) for all edges. Other

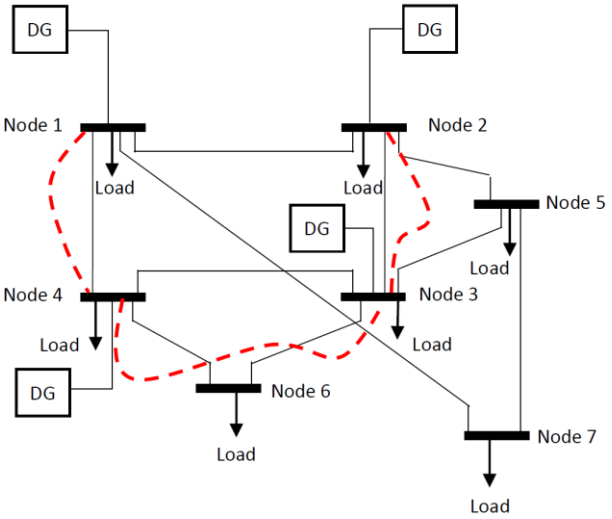

Fig. 3 Topology of DC microgrid. Loads are electric vehicle fleet. The dashed lines represent the communication network.

Table 1 DGUs parameters.

DGU	unit	1	2	3	4
R	mΩ	0.2	0.3	0.5	0.1
L	mH	1.8	2	3	2.2
C	mF	2.2	1.9	2.5	1.7
w	-	2	5	6	3
V^*	V	380	380	380	380

Table 2 Line parameters.

Start node	End node	R [mΩ]	L [μH]
1	2	80	2.1
2	3	70	2.3
3	4	100	2
1	4	80	1.8
1	7	90	3
2	5	80	2.1
3	5	70	2.3
5	7	110	2
3	6	80	1.8
4	6	90	1.9

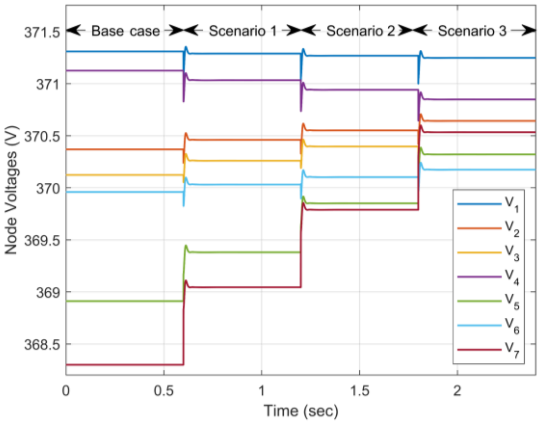

Fig. 4 Voltages at the different nodes of the microgrid subject to three different scenarios. Base case ($0 < t < 0.6$ s [14]), Scenario 1 (0.6 s $< t < 1.2$ s), Scenario 2 (1.2 s $< t < 1.8$ s), and Scenario 3 ($t > 1.8$ s).

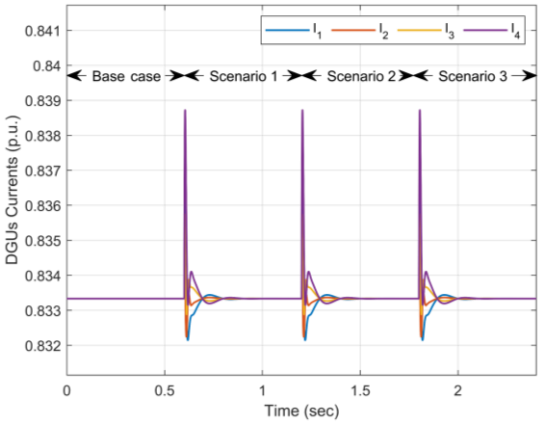

Fig. 5 Output currents of different DGUs in p.u. subject to three different scenarios. Base case ($0 < t < 0.6$ s) [14]), Scenario 1 (0.6 s $< t < 1.2$ s), Scenario 2 (1.2 s $< t < 1.8$ s), and Scenario 3 ($t > 1.8$ s).

parameters are considered as $K_i = 0.5$, $T_{\theta i} = 1$, and $T_{\varphi i} = 0.01$ for all nodes as in [14].

First, we consider a current demand as in Table 3. This situation is considered as the base case and the steady-state node voltages are reported (Column three in Table 3). Energy prices at different nodes are derived from (27) with $\alpha = 3$ and are also shown in Table 3.

To investigate the effectiveness of the proposed algorithm, three different performance metrics were considered:

1) The maximum deviation of node voltages defined by $f_{max\text{-}min}(V)$,
2) The minimum voltage of the nodes of the microgrid,
3) The power losses in the transmission network.

The first two metrics represent a measure of voltage regulation and the third metric represents the efficiency of the microgrid. These metrics were evaluated based on several scenarios:

- Base-case scenario: The same formulation as proposed in [14] is used. However, non-zero resistance in the RLC filter of DGUs and no price incentive is applied;
- Scenario 1: Only 33% of loads follow the incentive;
- Scenario 2: 66% of loads follow the incentive;
- Scenario 3: All loads follow the incentive.

In all scenarios, the total current demand is 150 A. Different current demands for different scenarios according to nodal prices in Table 3 are presented in Table 4.

To make these scenarios comparable, we run them in a single simulation. Our simulation starts at the base-case scenario, and then switches to Scenarios 1, 2, and 3 at $t = 0.5$ s, $t = 1.2$ s, and $t = 1.8$ s, respectively. Node voltages are shown in Fig. 4.

Based on Fig. 4 it can be observed that the voltage difference between nodes in scenarios 1 to 3 is much better than the base-case scenario. It can be seen that the steady-state voltage difference between nodes is

Table 3 Steady-state node voltages and energy price at different nodes.

Node number	Current demand [A]	Steady-state voltage [V]	Energy price [$]
1	15	371.31	1.074 Â
2	15	370.37	1.082 Â
3	15	370.12	1.085 Â
4	21	371.13	1.075 Â
5	30	368.91	1.096 Â
6	15	369.96	1.086 Â
7	39	368.30	1.102 Â

Table 4 Current demand in different scenarios.

Node number	Current demand scenario 1 [A]	Current demand scenario 2 [A]	Current demand scenario 3 [A]
1	10+14	5+28	42
2	10+9	5+18	27
3	10+6	5+12	18
4	14+12	7+24	36
5	20+3	10+6	9
6	10+4	5+8	12
7	26+2	13+4	6

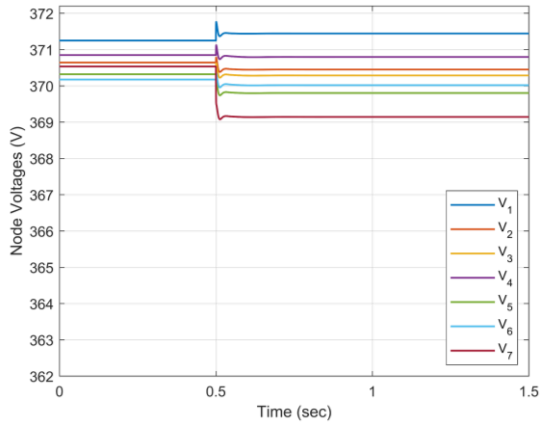

Fig. 6 Voltages at the different nodes of the microgrid subject to a line removal at time t = 0.5 s using the proposed model.

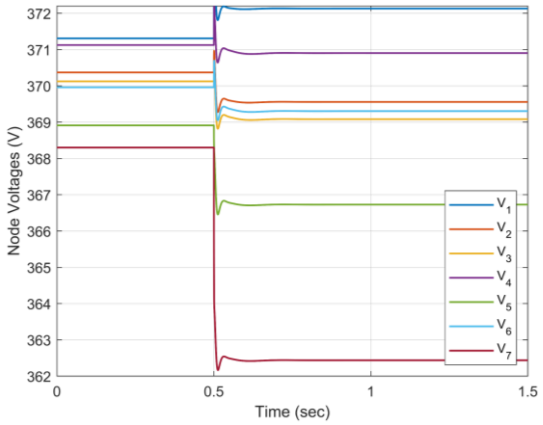

Fig. 7 Voltages at the different nodes of the microgrid subject to a line removal at time t = 0.5 s using the method proposed in [14].

gradually decreasing as more customers accept the offered price incentive. More precisely, steady-state $f_{max\text{-}min}(V)$ is equal to 3V in the base-case scenario, whereas it is 2.2 V , 1.5 V , and 1.1 V for scenarios 1 to 3, respectively. In addition, steady-state transmission power loss is 189 W in the base-case scenario and it reduced to 110 W, 55 W, and 22 W for scenarios 1 to 3, respectively. At the same time, the nominal voltage of the system is 380 V and the minimum node voltage is 368.3 V in the base-case scenario and it increased to 369 V, 369.8 V, and 370.2 V for scenarios 1 to 3, respectively. Therefore, it can be concluded that $f_{max\text{-}min}(V)$ and the transmission power loss are reduced and minimum node voltage increase as moving loads accept the proposed price incentive.

Table 5 summarizes the performance measures of different scenarios and the results of paper [14] with nonzero resistance in the RLC filter of DGUs. These simulations show that the energy pricing in different nodes of the microgrid leads to a) a much better voltage profile in the system, b) a less power dissipation and c) a higher minimum node voltage in the network with respect to [14]. At the same time, the current generated by each DGU converges to the desired values and proportional current sharing is achieved, as shown in Fig. 5.

Figs. 6 and 7 illustrate the comparison results of the effect of failure in the system network using the proposed method (scenario 3) and the method proposed in [14] when the line between node 1 and node 7 is removed (Fig. 3) at time t = 0.5 s. From Figs. 6 and 7 it can be concluded that the minimum node voltages at steady-state in the proposed method decreases from 370.17 V to 369.14 V and the steady-state node voltage deviation ($f_{max\text{-}min}(V)$) increases from 1.1 V to 2.3 V after failure in the network (please refer to Table 6). However, the minimum node voltages at steady-state using method proposed in [14] decreases from 368.3 V to 362.4 V and the steady-state node voltage deviation ($f_{max\text{-}min}(V)$) increases from 3 V to 9.7 V after failure in the network. Disseminating the loads from node 7 to other nodes according to the high price of node 7 is the reason that makes the proposed method outperform the previous method in the literature (such as [14]).

6 Conclusions

This study proposed a method to improve the problem of voltage regulation in DC microgrids. The proposed method is based on a load management approach on the demand side.

In the proposed algorithm, the voltage of each node was considered as a measure to define the energy price offered to the moving nodes (e.g. EVs) connected to that node. Node-specific energy prices were used as a strong incentive to manage loads of systems across the grid. The simulation results showed that the proposed method was able to successfully tackle the voltage regulation problem in DC microgrids and it is robust in network failure. In other words, the voltage deviation is improved from 3 V to 1.1 V, transmission power loss

Table 5 Steady-state $f_{max\text{-}min}(V)$, minimum node voltage, and power losses at different scenarios.

	$f_{max\text{-}min}(V)$ [V]	Power loss [W]	Minimum node voltage [V]
Base-case Scenario [14])	3	189	368.3
Scenario 1	2.2	110	369
Scenario 2	1.5	55	369.8
Scenario 3	1.1	22	370.2

Table 6 Minimum steady-state node voltages, and steady-state voltage deviation $f_{max\text{-}min}(V)$ subject to line removal.

	Proposed method		Reference [14]	
	Before fault	After fault	Before fault	After fault
Minimum node voltage	370.17	369.14	368.30	362.44
$f_{max\text{-}min}(V)$	1.1	2.3	3	9.7

reduced from 189 W to 22 W, and finally, the minimum node voltage upgraded from 368.3 V to 370.2 V as moving loads accept the proposed price incentive.

In this paper, we have investigated the problem of load management for grid voltage regulation. The penetration rate of electric vehicles for load management and the existence of battery energy storage systems is another interesting issue that could form the future direction of similar studies. As a result, the suitable placement of manageable loads on one side and the existence of other fast response sources such as BESS on the other side are still open questions that need more investigation in future works. Furthermore, the optimal capacity and optimal placement of BESS in these grids are interesting challenges for the future direction of the current paper.

References

[1] A. T. Elsayed, A. A. Mohamed, and O. A. Mohammed, "DC microgrids and distribution systems: An overview," Electric Power Systems Research, Vol. 119, pp. 407–417, 2015.

[2] A. Cherukuri and J. Cortes, "Distributed coordination of DERs with storage for dynamic economic dispatch," *IEEE Transactions on Automatic Control*, Vol. 63, No. 3, pp. 835–842, 2017.

[3] R. H. Lasseter and P. Paigi, "Microgrid: A conceptual solution," in *IEEE 35th Annual Power Electronics Specialists Conference*, Vol. 6, pp. 4285–4290, 2004.

[4] J. M. Guerrero, P. C. Loh, T. L. Lee, and M. Chandorkar, "Advanced control architectures for intelligent microgrids—Part II: Power quality, energy storage, and AC/DC microgrids," *IEEE Transactions on Industrial Electronics*, Vol. 60, No. 4, pp. 1263–1270, 2012.

[5] M. Shahidehpour, "Perfect power prototype for Illinois institute of technology," *Illinois Institute of Technology*, Chicago, IL, United States, 2014.

[6] A. M. Amani, N. Gaeini, M. Jalili, and X. Yu, "Which generation unit should be selected as control leader in secondary frequency control of microgrids?" *IEEE Journal on Emerging and Selected Topics in Circuits and Systems*, Vol. 7, No. 3, pp. 393–402, 2017.

[7] J. J. Justo, F. Mwasilu, J. Lee, and J. W. Jung, "AC-microgrids versus DC-microgrids with distributed energy resources: A review," *Renewable and Sustainable Energy Reviews*, Vol. 24, pp. 387–405, 2013.

[8] P. Kundur, N. J. Balu, and M. G. Lauby, *Power system stability and control*. New York: McGraw-Hill, 1994.

[9] S. Anand, B. G. Fernandes, and J. Guerrero, "Distributed control to ensure proportional load sharing and improve voltage regulation in low-voltage DC microgrids," *IEEE Transactions on Power Electronics*, Vol. 28, No. 4, pp. 1900–1913, 2012.

[10] M. Cucuzzella, S. Trip, C. De Persis, X. Cheng, A. Ferrara, and A. van der Schaft, "A robust consensus algorithm for current sharing and voltage regulation in DC microgrids," *IEEE Transactions on Control Systems Technology*, Vol. 27, No. 4, pp. 1583–1595, 2018.

[11] N. Noroozi, S. Trip, and R. Geiselhart, "Model predictive control of DC microgrids: current sharing and voltage regulation," *IFAC-Papers OnLine*, Vol. 51, No. 23, pp. 124–129, 2018.

[12] M. Tucci, S. Riverso, and G. Ferrari-Trecate, "Line-independent plug-and-play controllers for voltage stabilization in DC microgrids," *IEEE Transactions on Control Systems Technology*, Vol. 26, No. 3, pp. 1115–1123, 2017.

[13] M. Tucci, L. Meng, J. M. Guerrero, and G. Ferrari-Trecate, "Stable current sharing and voltage balancing in DC microgrids: A consensus-based secondary control layer," *Automatica*, Vol. 95, pp. 1–13, 2018.

[14] S. Trip, M. Cucuzzella, X. Cheng, and J. Scherpen, "Distributed averaging control for voltage regulation and current sharing in DC microgrids," *IEEE Control Systems Letters*, Vol. 3, No. 1, pp. 174–179, 2018.

[15] J. Zhao and F. Dorfler, "Distributed control and optimization in DC microgrids," *Automatica*, Vol. 61, pp. 18–26, 2015.

[16] M. Tucci, L. Meng, J. M. Guerrero, and G. Ferrari-Trecate, "A consensus-based secondary control layer for stable current sharing and voltage balancing in DC microgrids," *arXiv preprint arXiv:1603.03624*, 2016.

[17] M. Cucuzzella, S. Trip, and J. Scherpen, "A consensus-based controller for DC power networks," *IFAC-Papers OnLine*, Vol. 51, No. 33, pp. 205–210, 2018.

[18] C. De Persis, E. R. Weitenberg, and F. Dorfler, "A power consensus ¨ algorithm for DC microgrids," *Automatica*, Vol. 89, pp. 364–375, 2018.

[19] F. Dorfler and F. Bullo, "Kron reduction of graphs with applications to electrical networks," *IEEE Transactions on Circuits and Systems I: Regular Papers*, Vol. 60, No. 1, pp. 150–163, 2012.

[20] S. Y. Caliskan and P. Tabuada, "Towards Kron reduction of generalized electrical networks," *Automatica*, Vol. 50, No. 10, pp. 2586–2590, 2014.

[21] R. Han, H. Wang, Z. Jin, L. Meng, and J. M. Guerrero, "Compromised controller design for current sharing and voltage regulation in DC microgrid," *IEEE Transactions on Power Electronics*, Vol. 34, no. 8, pp. 8045–8061, 2018.

[22] R. Palma-Behnke, C. Benavides, E. Aranda, J. Llanos, and D. Saez, "Energy management system for a renewable based microgrid with a demand side management mechanism," in *IEEE Symposium on Computational Intelligence Applications in Smart Grid (CIASG)*, pp. 1–8, 2011.

[23] D. Li, W. Y. Chiu, and H. Sun, "Demand side management in microgrid control systems," *Microgrid. Elsevier*, pp. 203–230, 2017.

[24] G. Aghajani, H. Shayanfar, and H. Shayeghi, "Demand side management in a smart micro-grid in the presence of renewable generation and demand response," *Energy*, Vol. 126, pp. 622–637, 2017.

[25] X. Yang, Y. Zhang, H. He, S. Ren, and G. Weng, "Real-time demand side management for a microgrid considering uncertainties," *IEEE Transactions on Smart Grid*, Vol. 10, No. 3, pp. 3401–3414, 2018.

[26] S. S. Kia, B. Van Scoy, J. Cortes, R. A. Freeman, K. M. Lynch, and S. Martinez, "Tutorial on dynamic average consensus: The problem, its applications, and the algorithms," *IEEE Control Systems Magazine*, Vol. 39, No. 3, pp. 40–72, 2019.

[27] A. Karimpour, R. Asgharian, and O. Malik, "Determination of PSS location based on singular value decomposition," *International Journal of Electrical Power & Energy Systems*, Vol. 27, No. 8, pp. 535–541, 2005.

[28] A. Karimpour, O. Malik, and R. Asgharian, "Singular value decomposition as a measure for control structure design in power systems," *Electric Power Components and Systems*, Vol. 32, No. 3, pp. 295–307, 2004.

[29] C. T. Chen, *Linear system theory and design*. 3rd Ed. New York: Oxford University Press, 1999.

A. Karimpour received his Ph.D. in Control Engineering from the Ferdowsi University of Mashhad, Iran. He is currently an Associate Professor with the Faculty of Engineering, Ferdowsi University of Mashhad, Iran. His current research interests include dynamical systems, power systems, and microgrids.

A. M. Amani (M'16) has completed Graduate and Post-Graduate studies all in Electrical Engineering (Control Systems). He is now with the School of Engineering at Royal Melbourne Institute of Technology (RMIT University), Melbourne, Australia. His research interests include fault-tolerant control systems, control of complex networks and spectral graph theory, and stability and control of future power systems.

M. Karimpour received his B.Sc. and M.Sc. degrees in Electrical Engineering, and he is currently a Ph.D. student in Electrical Engineering at the University of Melbourne. He has several years of experience in various power generation industries covering thermal and wind power plants. His research interests are in the field of control system design and its applications to wind turbines, power electronics and power system stability.

M. Jalili (M'09–SM'16) received the Ph.D. degree in Computer and Communications Sciences from the Swiss Federal Institute of Technology Lausanne, Lausanne, Switzerland, in 2008. He was an Assistant Professor with the Sharif University of Technology, Tehran, Iran. He is currently a Senior Lecturer with the School of Engineering, RMIT University, Melbourne, VIC, Australia, and was the Australian Research Council DECRA Fellowship and RMIT Vice-Chancellor Research Fellowship. His current research interests include network science and dynamical systems.